Modelling the movement and wave impact of a floating object using SPH

Modelling the movement and wave impact of a floating object using SPH

Johan Vandamme[1]; Dr Qingping Zou[1]; Prof Dominic Reeve[1]; Dr Yali Zhang[1]

[1] Centre for Coastal Dynamics and Engineering, School of Engineering, University of Plymouth, UK.
Fax: +44 (0)1752 232638. E-mail: johan.vandamme@plymouth.ac.uk

Abstract

This paper investigates fluid and floating object interaction using a novel adaption of the Smoothed Particle Hydrodynamics (SPH) method. This problem is significant to reducing the difficulties of cost-effective designs of wave energy converters, offshore and coastal structures. In particular, this paper investigates water impact, hydrodynamic forces, fluid motions and movement of the object in typical cases of object entry and exit from still water and movement within a surf zone. Conventional grid based models, such as FEM and FDM, are required to generate or adapt the inbuilt mesh at each timestep to conform to the movement of the free surface and the object. SPH is a Lagrangian particle method which does not require a grid, therefore, it is a robust method with which to tackle the problem. The water impact pressure prediction, traditionally considered one of the weaker facets of SPH, shows good agreement with published experimental and numerical results. The hydrodynamic forces exerted on the object, and hence the movement of the object itself, are well predicted. The velocity field of the fluid domain is also captured well. The diversity and results of the case studies provide a good foundation to evaluate the accuracy and stability of using SPH to model the interaction between floating objects and free surface flow, and subsequently to evaluate wave energy capture devices.

Keywords: SPH, floating object, wave energy converter, wave loading, free surface flow, water exit

Nomenclature

SPH = Smoothed Particle Hydrodynamics
WCSPH = Weakly Compressible SPH
ISPH = Incompressible SPH

1 Introduction

The increasing demand for energy combined with the increased sensitivities to climate change and carbon emissions have resulted in a significant amount of research into renewable resources that has greatly advanced many areas of green energy capture. Wave energy converters (WECs) are one of these areas, and show promising potential. Due to the nature of WECs, they are placed in locations with highly non-linear wave movement, and their movement is often complex and violent, including significant quantities of exit and re-entry into the fluid domain. Numerically modelling of this entry and exit, as well as capturing the slamming force of a floating object is critical to the design and optimisation of wave energy devices, and a particle method is herein developed to model these phenomena.

Although there are many methods of numerical simulation for wave dynamics, including the modelling of floating objects, [5-7] the traditional methods of modelling are grid based or continuous in their methodologies. This means that computational difficulty is markedly increased when phenomena such as surface separation, piercing, joining or large differential movement is involved in the simulation. As a result of this it becomes challenging to accurately capture the movement and fluid response to a WEC.

The increasing computational power that is available to researchers has meant that methods could progress beyond efficient grid-based methods of modelling. The computational method presented in this paper is particle based; allowing it many of the benefits denied the more traditional methods. Developed for the study of astrophysics, Smoothed Particle Hydrodynamics (SPH) [8, 9] has been adapted for free surface flows and a diverse manner of hydrodynamic phenomena [10-12]. An extra module has been developed and used to simulate the movement of solid bodies within the fluid domain. The object is made up of solid boundary particles, their local positions fixed relative to each other, and their global positioning dependent on the hydrodynamic forcing of the water particles which act normally to the obstacle surface. This novel approach allows modelling to widen the scope to many more types of problems than traditional methods. A selection of test cases are presented below, examining the results behind a number of fundamental phenomena within the research area of floating object movement.

2 SPH Modelling

The mathematical basis for the SPH method is modelling particles whose interactions are based on the Navier-Stokes equations. The representation of the fluid domain as particles therefore allows a computational domain with no grid and no oppressive structure; ergo, unlike Eulerian models, it does not become unstable when the case involves large relative or inconsistent displacement, distortion, or separation and combination of fluid bodies.

Every particle within the domain is assigned scalar parameters that include mass, pressure, velocity components and so on. This data set of the domain can then be interpolated using the following equation to computer any one of the scalar quantities *f(x)* for any given particle:

$$f(x) = \sum_j f_j W(x - x_j) V_j \tag{1}$$

V_j here is the volume of the particle, explicitly computed by its density as each particle has a fixed mass. The smoothing function $W(x-x_j)$ is known as the kernel function, and this can be one of a selection of smoothing functions which have various shapes (quadratic, Gaussian, cubic, etc) and acts as a weighted average for the summation of particles. Although many of these kernels would theoretically extend to infinity, meaning every particle within the fluid domain affects the values for every other particle, this zone of interaction is restricted to particles separated by a distance of less than *2h*, where *h* is a user defined parameter. This allows for more efficient modelling and vastly reduces the computational time needed.

The conservation of momentum and mass, as seen in Monaghan [11], is applied to the particle a in the form:

$$\frac{dv_a}{dt} = -\sum_j m_j \left(\frac{p_a}{\rho_a^2} + \frac{p_j}{\rho_j^2} + \prod_{aj}\right)\nabla_a W_{aj} + g \tag{2}$$

$$\frac{d\rho_a}{dt} = \sum_j m_j (v_a - v_j).\nabla_a W_{ab} \tag{3}$$

Where *j* is all other particles within the radius of *2h*, p_j is the pressure; v_j is the velocity; m_j the mass and ρj the density of particle *j*. $\prod_{aj}$ is an empirical approximation of the viscosity effects [11] and W_{aj} is the kernel function.

The conservation of mass is applied by ensuring volume change is simulated through altering the density of the particle *a*, so that, providing no particles enter or leave the domain, mass is kept constant. The free surface particles are easily found within the computational domain, and the numerical averaging does not lower the densities within *2h* of the free surface.

Monaghan [13] developed the XSPH correction which ensures particles in close proximity move with a similar velocity within each timestep, avoiding overlapping of the particles and subsequent errors. Monaghan [12] amongst others, [14, 15] have also researched into further correcting the tensile instability inherent in some SPH simulations, which has since been integrated into the kernel function.

Boundary conditions of SPH simulations are met in the form particles with a fixed position which exert repulsive forces against any fluid particles if they move to within a specified radius of the boundary. The two main approaches of modelling the boundary particles are set out by Monaghan [11] and Dalrymple [16].

More information about the developments of SPH, which has been highly pursued at Johns Hopkins University, can be found in [17], including the inclusion of sub-grid scaling and Shepard filtering allowing for more accuracy in turbulent flow conditions. As detailed in [18], sub-particle scale turbulence can be modelled with no need for using a second-order derivative, saving computational time and increasing stability [19].

In addition to Weakly Compresible SPH (WCSPH), the SPH method has also been adapted to a fully incompressible method (ISPH). Although ISPH tends to predict pressure fluctuations more accurately, the results of both methods are comparable. Runtimes are also similar, as the ISPH method takes longer per timestep but will use larger time steps throughout the run. WCSPH allows for a higher resolution for a given memory size [20]. The method used by the authors is that of WCSPH, developed from the open-source SPHysics code published on the University of Manchester website [21].

The mechanics of floating object modelling within the SPH simulation has been achieved by using boundary particles to construct the shape of the object in question. Contrary to the method employed by [22] this allows a homogeneous method of computation, increasing the efficiency of the model

The movement of the obstacle into the fluid domain triggers movement within the fluid particles that is handled by the existing SPH simulation. In addition to this, the obstacle can also be anchored by one or multiple two-phase linear springs, allowing restricted movement in a dynamic fluid domain.

3 Results

3.1 Wedge Entry

Results are presented below for initial test cases of the floating object simulations. The first case is a simple 2D wedge drop first published by Greenhow [23], who plunged wedges of varying deadrise angles through the water surface at a $2ms^{-1}$, capturing the surface elevation and slamming coefficient. The wedges varied in their dead rise angle, and the result of the SPH simulation using wedges of 30^o and 45^o angles can be qualitatively compared to the results published.

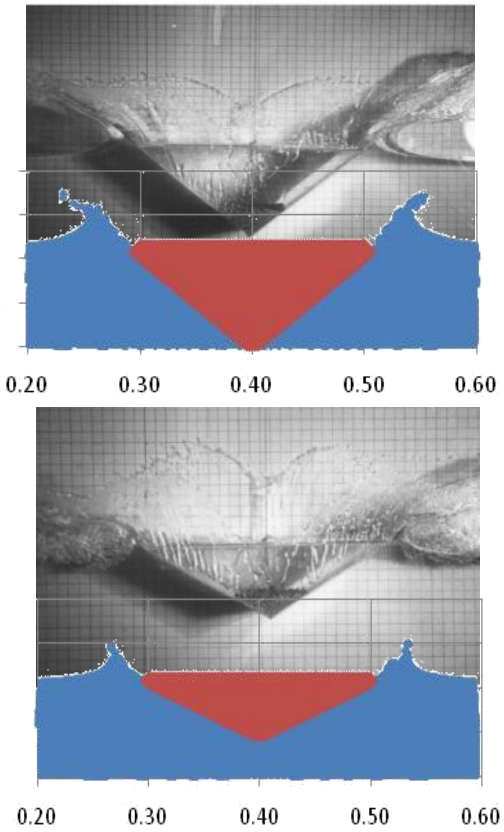

Figure 1: Comparison of SPH (colour) and the results of Greenhow(black and white) for a controlled plunging of a wedge with a 45^o (top) and a 30^o (bottom) deadrise angle.

Fig. 1 above demonstrates the suitability of SPH for moving object modelling. The general trends of the jets are reproduced well considering the resolution of the solution. Another advantage of using SPH in simulations such as this is the ability to allow for fluid separation, such as spray, as seen on the left-hand side of the 45^o wedge. This phenomena is much more complex for a computational method that uses grids or meshes in place of particles.

Although these wedges were plunged into the fluid domain with a fixed velocity, work has also been done where only the entry velocity has been defined, and the subsequent movement is then a result of the water forces on the wedge. There are plenty of examples of physical and theoretical testing around the subject area of wedge slamming, which is important to not only the renewable energy industry but also the shipping and ocean transport industry. Aside from Greenhow [23], extensive work has been carried out by Zhao and Faltinsen [2, 24] considering the entry of arbitrary 2D bodies, as well as the impact study of Cointe [25] and the detailed vertical and oblique entry of wedges presented by Judge et al [26]. This test has been done with an entry velocity of $6.15ms^{-1}$, and the results are compared to those published by Shao [1] who used ISPH with a similar resolution. The results show water surface, vector plots and pressure contours for the time following the initial impact.

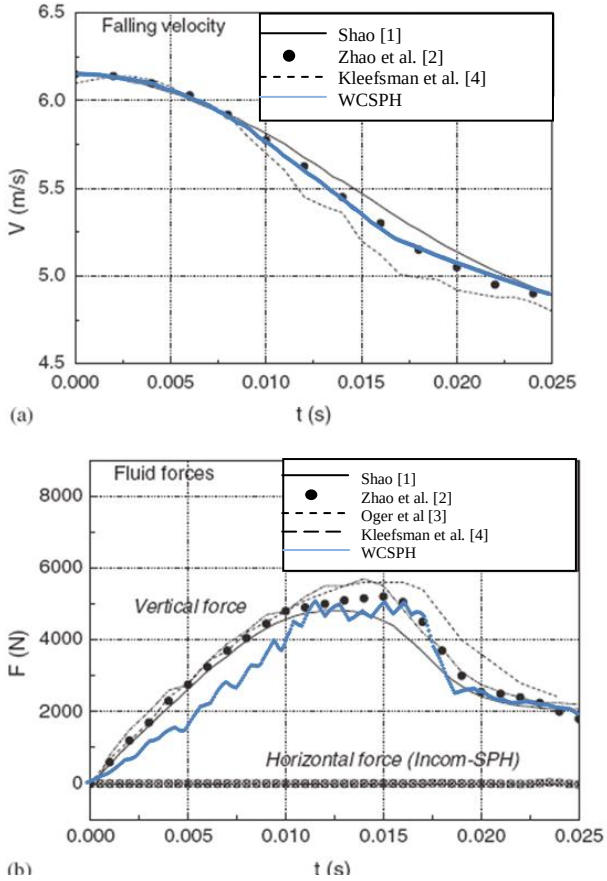

Figure 2. (a) The falling velocity of a wedge with a 30^o dead rise angle, timed from the moment of initial impact.
(b) The vertical force exerted on the wedge by the fluid body. Authors results (WCSPH)in blue plotted on graph from [23]

Figure 2 shows the close correlation between the weakly compressible SPH results and the existing results. The velocity figure shows the results give a smoother profile than the results shown by Kleefsman [4], and the trend sits comfortably within data points measured by Zhao et al [2], with a slight inaccuracy presented by the slightly larger deceleration towards t=0.025s.

The second graph shows a good prediction of the pressure, a factor that is often considered the least accurate parameter of weakly compressible SPH.

Although the initial rise in upwards force seems languid in comparison to the other results, the peak and residual forces are predicted correctly and the profile of the results are well matched. The slight oscillations within the results are likely to be the result of slight feedback resulting from the time step and sound wave speed used.

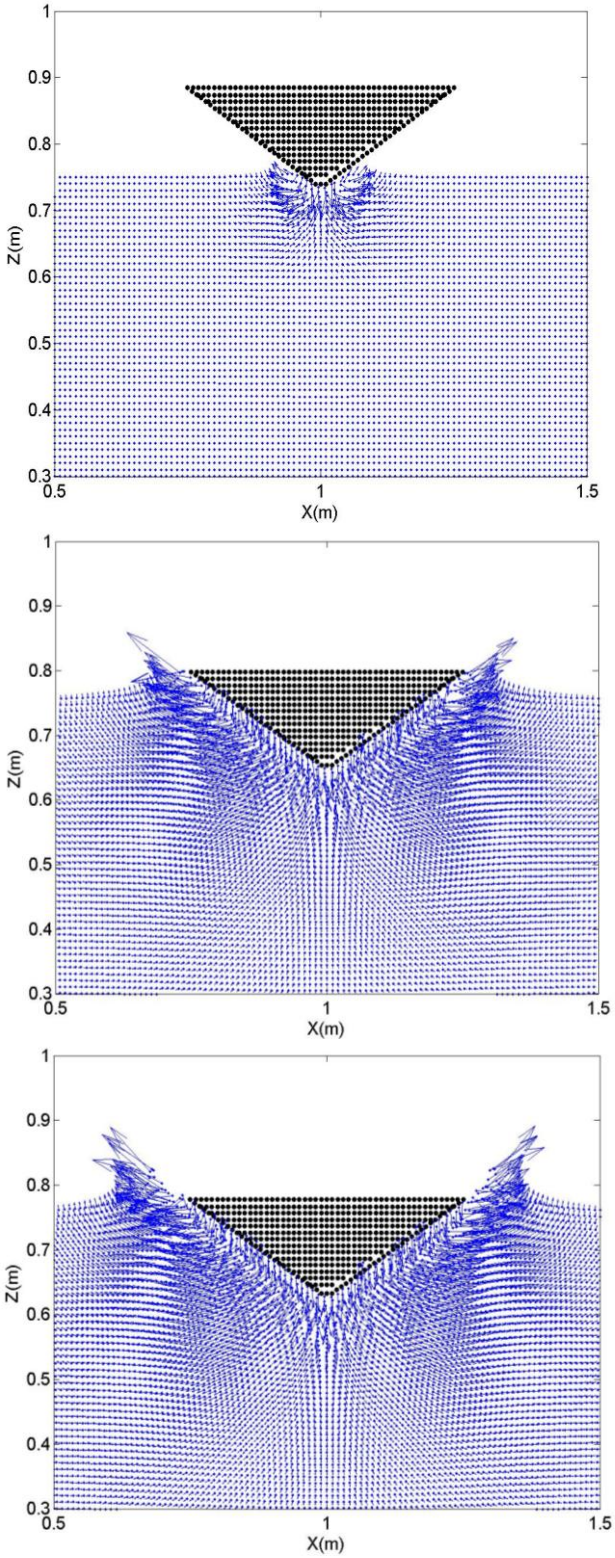

Figure 3. The velocity plot for the fluid domain at times 0.004s, 0.016s and 0.02s. The jets as described in Greenhow [23] can be clearly seen.

Figure 3 shows a sequence of images with a wedge of a 30^o deadrise angle. The initial penetration into the surface causes the fluid to move down and to the side of the incoming wedge. These jets are attached to the wedge surface and propagate further up as the wedge progresses deeper into the fluid domain. Eventually the jets detach from the wedge surface and shot to the side as seen in the final image. The maximum velocity of the jets is 17.1ms^{-1} in the final image, from an initial point of 15.8ms^{-1} in the second image. These values compare well with the values predicted numerically with the previous research.

Although it is traditionally viewed as one of the weaknesses of weakly compressible SPH, the pressure induced under the wedge can be compared with the ISPH results, as shown in Figure 4. The two sets of data were computed using identical particle sizes (resolution), although the differences in appearance of the results are because the author has not interpolated the shading on the weakly compressible values.

The upper image of Figure 4 clearly shows a bulb of high pressure under the initial impact of the wedge, with no disturbance to the fluid further afield. The maximum pressure under the wedge is in the region of 100kPa. This area of high pressure diffuses as the water moves upwards and sideways along the wedge, as shown in the second figure where the maximum pressure is around 70kPa.

An obvious discrepancy between the two sets of results is displayed in the second image of Figure 4, where the surface profile of the ISPH model already displays some splashing and a more significant jet formation than the authors' results, which show a more uniform result with a later jet formation giving a more powerful result.

The numerical diffusion of the jets makes accurate predictions of jet volume complex, so it is difficult to know which result is more accurate. However, the authors result is more powerful than the ISPH which are understood to be significantly weaker than those found in Oger et al [3], who used a complex radial spacing and a fine resolution near the surface to try to predict the jets accurately.

The results of the 30^o wedge entry show the performance of a normally configured weakly compressible SPH to predict the fluid forces upon an object and also the forces within the fluid domain itself. This is a crucial step to fully modelling a floating object within the fluid domain when there can be exit and/or entrance into the fluid surface.

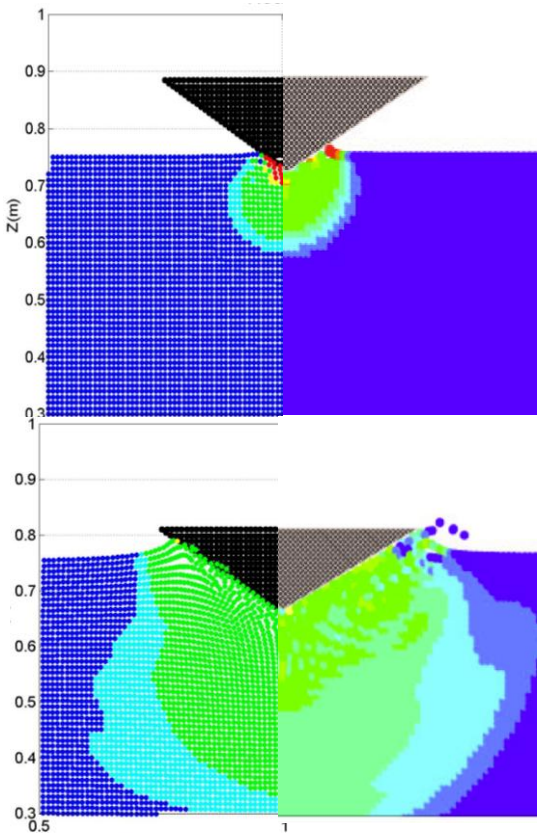

Figure 4 –Pressure under the impact of the wedge with weakly compressible SPH on the left hand side and the results of Shao[1] on the right.

Although there is less research available to compare to, the authors also examined the slamming coefficient for various wedge angles. Figure 5 shows some preliminary results of slamming coefficients.

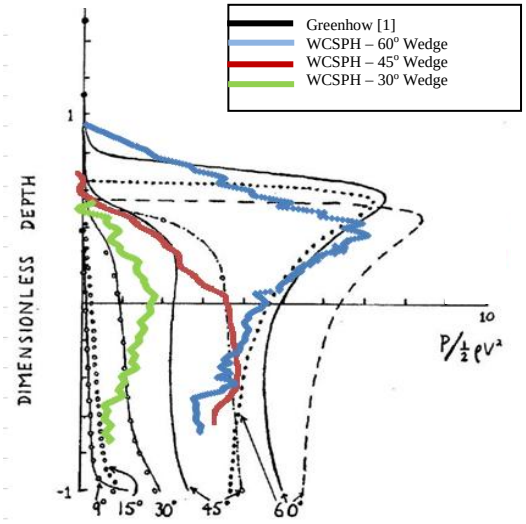

Figure 5 – Slamming coefficient against dimensionless depth for 2D wedges plotted over the predicted values from Greenhow [23]

The slamming coefficient graph above compares the free motion results for wedges of 30°, 45° and 60°. The results differ slightly from the numerical solution, but there is clear indication that the SPH model tends towards the expected solution.

3.2 Object exit

When considering the modelling of floating objects within a fluid domain, the exit of an object from the fluid domain is as critical to model as the behaviour of an obstacle. However, much less work has been published about this phenomenon and so there is less comparative data available.

When a cylinder is submerged into the fluid domain and allowed to rise to the surface, the free surface deformation has been presented by Greenhow [27] and is compared to the SPH numerical results.

The free surface deformations for a 0.5 diameter cylinder with a density of 1000kgm^{-3} are presented at comparable time steps to the numerical results [27] and are shown in figure 6. In this case, the cylinder is given a constant and motion of 1ms^{-1} vertically upwards, and the particle size was 0.02m.

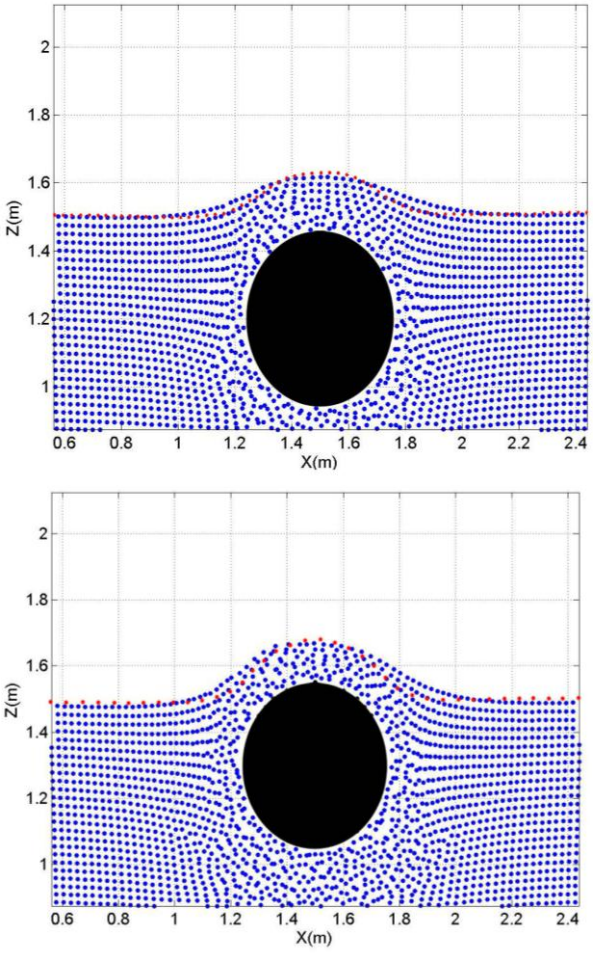

Figure 6 - Free surface deformation due to a cylinder rising through the free surface, for dimensionless time (T=Ut/d) of 0.4 and 0.6. Red dots show the numerical results presented in Greenhow and Moyo [27]

Figure 6 shows good correlation with the results, predicting the peak over the rising cylinder correctly. The SPH results do give a wider raised area than the

numerical results in [27] and at this stage it is unclear why this discrepancy occurs. However, the general shape is well matched by both frames.

When considering true motion of the cylinder through the fluid, it is important to consider a cylinder whose movement, resulting from the fluid forces, is unbounded. In this case, a cylinder of the same diameter was given a density of 250kgm^{-3}, and initially set up with its centre 0.5m below the still water surface which was at 1.5m

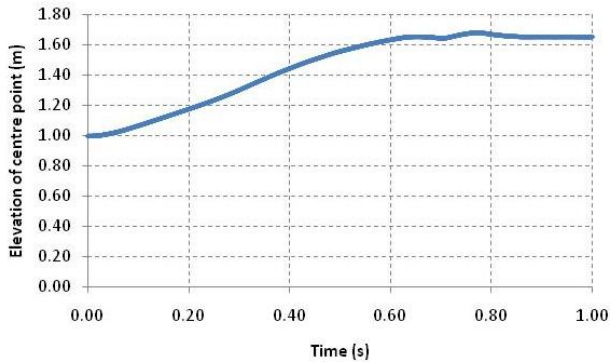

Figure 7 – Elevation of a cylinder submerged 0.5m below the free surface and allowed to rise to equilibrium point

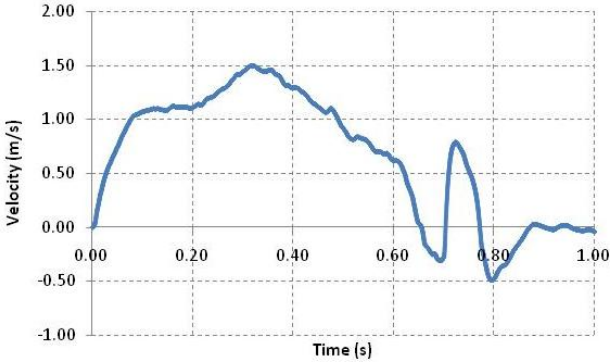

Figure 8 –Velocity of a cylinder submerged 0.5m below the free surface and allowed to rise to equilibrium point

Fig. 7 clearly shows the obstacle rising through the surface until it reaches the expected equilibrium depth. Although the calculated centre depth by displacement would be at 1.6m exactly, it is possible that the slight extra height is achieved by the upthrust of the residual eddies, which can be seen in Fig 9.

Fig. 8 shows an initial upthrust caused by the hydrostatic pressure, which levels out at around 0.08 seconds. This velocity increases again as the free surface is pushed higher than the still water depth, increasing the lateral force for the fluid above the cylinder as it moves sideways away from the obstacle under gravity. The velocity then decreases and a slight oscillation can be seen before the obstacle reaches equilibrium.

Figure 9 show the fluid movement around the cylinder. One of the side-effects of the particle method is that when a fluid particle becomes separated from the rest of the domain it will be affected only by gravity, causing it, occasionally, to have a disproportionate effect on the domain when it rejoins it. This can be seen in the figures below as the fluid above the obstacle became separated from the domain earlier on the left hand side than it did on the right, and thus the asymmetries within the results appear disproportionate to the initial cause.

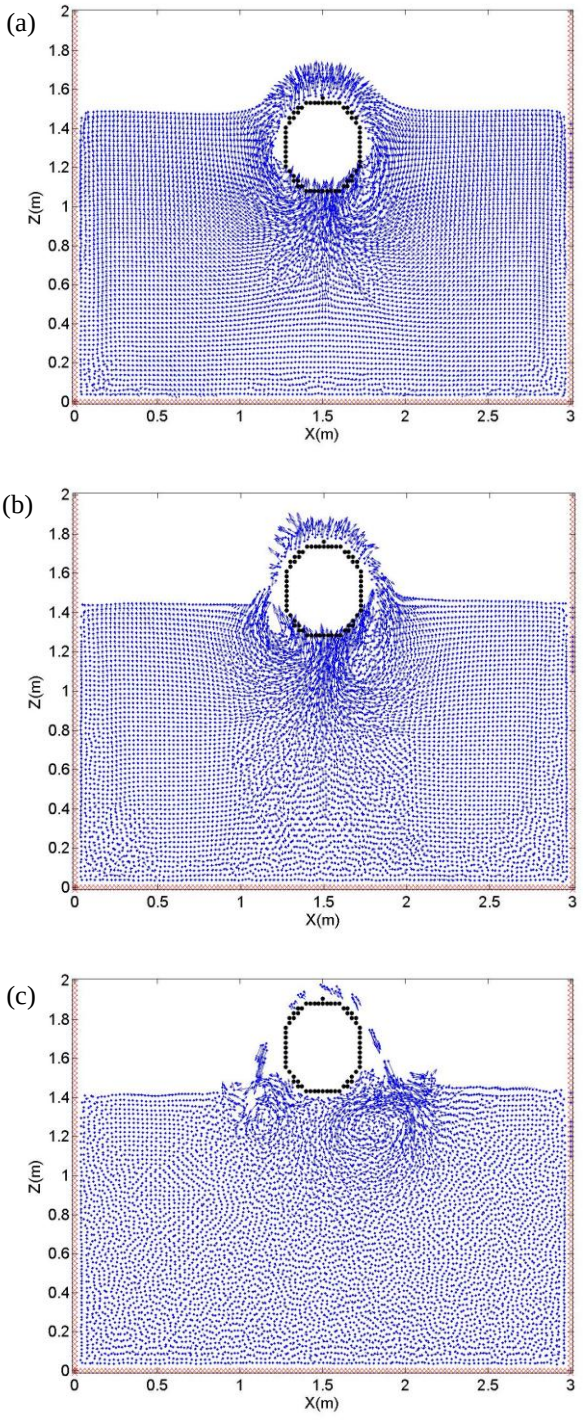

Figure 9 – Velocity plots of the fluid domain as the cylinder rises through the fluid (a), breaches the surface (b), and as the cylinder comes to rest (c).

The top figure within Fig. 9 clearly shows the water flowing around the cylinder in a similar manner as is predicted for a forced movement. The fluid on top of the cylinder moves upwards at the same speed as the cylinder and outwards where there is no water pressure to prevent this. The space left by the cylinder is quickly filled with water flowing down from the sides, creating the eddies that can be seen propagating through the sequence of images.

The slight asymmetry observed is due to the discrete nature of SPH, whereby the particles are not automatically aligned with the central axis, and subsequently the fluid response varies. Decreasing the particle size would reduce the asymmetric response and ergo the model would converge to a symmetric profile, given sufficient computational time.

The middle image shows the particle separation on the left hand side whilst the right has a larger flow into the fluid domain, increasing the eddy below. This asymmetry is likely to be caused by a compounding of the initial asymmetry. Although this does produce inconsistent results, such discrepancies can be reduced with more particles in the computational domain.

3.3 Floating objects under wave action

Some initial investigations have been carried out regarding the movement of a cylindrical object when subjected to wave moment. A circular object was placed in the centre of the domain 3 metres from the wave paddle and 2 metres from a dissipative beach. The water depth was 1.0 meters and the waves had a period of around 2s and a height of 0.2m.

Figure 10 shows a vector plot of the obstacle under the wave at three time steps. The water movement deflected by the obstacle can be clearly seen, and the effect of the obstacle on the fluid on the shoreward side of the wave is also well displayed.

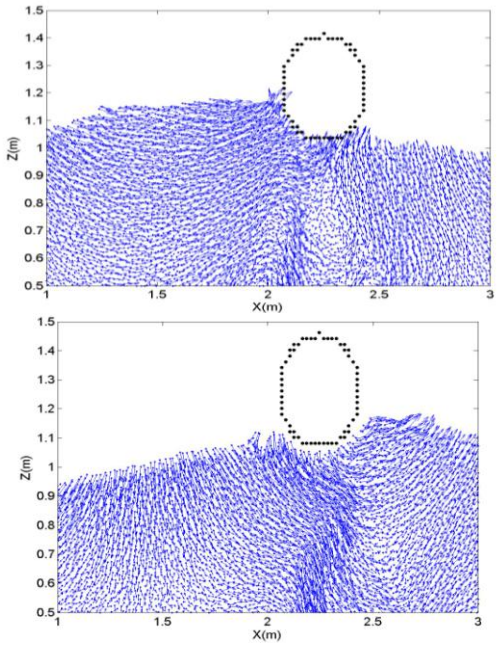

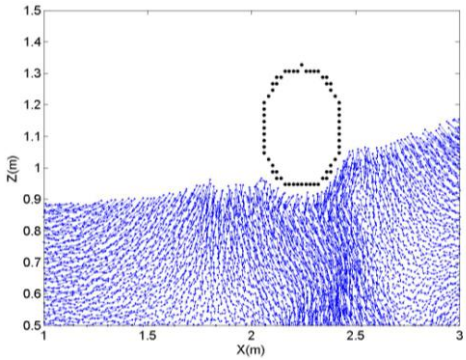

Figure 10 – Velocity plots of the fluid domain as the incoming wave reaches the floating object. The frames are separated by t=0.3 seconds.

The movement of the obstacle and the force exerted upon it are also captured by the simulation and the horizontal force is displayed in Fig 11. This clearly shows the phase of the wave movement around the obstacle. The obstacle was anchored in place to prevent it from significant lateral deviation. The numerical anchor used was a two phase linear spring, with zero stiffness for an anchor extension of up to 0.1m before a high stiffness correcting any movement of the obstacle further than this.

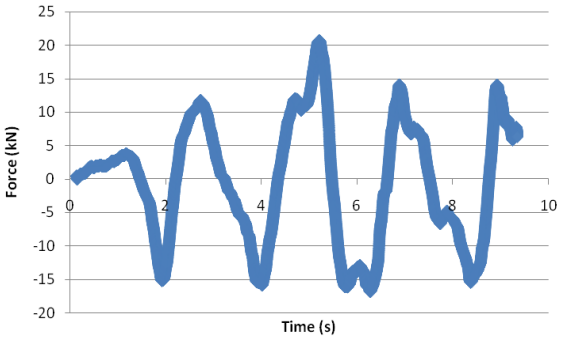

Figure 11 – Lateral hydrodynamic forcing on the cylinder over several typical wave cycles.

4 Conclusions and discussion

The research outlined in the paper has shown the suitability of weakly compressible SPH to model floating object movement within a fluid domain. SPH is a computationally intensive method of modelling, however all tests were completed on a single core of a 2.4GHz processor of a standard desktop computer, with run times less than 18hours. Further developments towards a GPU version of SPH will dramatically cut the computation time of further simulations, however. The results achieved are accurate within reasonable tolerances, and accuracy will be improved as work continues. Phenomena that are traditionally complex to simulate correctly, such as surface piercing and impact pressures have been modelled successfully.

The initial work has clearly demonstrated the potential for modelling the movement of floating objects. The drawbacks of the particle nature of SPH method are easily outweighed by the capabilities of it to easily model situations involving complete

submergence, emergence, and equilibrium. The water impact, movement, and forces upon the object have been well predicted in all test casts. Another advantage of SPH is the simplicity of extracting the data needed to for comparisons and design. The work presented above forms a solid grounding from which further exploration of application of the particle method to floating objects can be based. The results of such modelling by virtue of its explicit solutions will contribute to the design and understanding of wave energy devices.

To fully exploit the opportunities provided by the SPH method of modelling, this research direction should be pursued. Further work should include more detailed modelling of single or multiple objects within the fluid domain, and the air interaction within SPH which has received some attention in [28] . As demonstrated, the interaction of waves and floating bodies is complex and challenging, but the initial results presented in this paper are encouraging and show potential in this area of research. The fluid modelling ability of SPH for these situations is well tested and documented [10, 29].

Acknowledgements

The authors wish to thank Plymouth University for funding and providing this research opportunity, and are grateful for the support of the South West of England Regional Development Agency through PRIMaRE. The authors would also like to acknowledge the support of the Natural Environmental Research Council (Grant No. NE/E002129/1) during this project.

References

[1.] Shao, S., *Incompressible SPH simulation of water entry of a free-falling object.* International Journal for Numerical methods in Fluids, 2009. **59**(1): p. 25.

[2.] Zhao, R., O. Faltinsen, and J. Aarsnes, *Water entry of arbitrary two-dimensional sections with and without flow separation*, in *Twenty-first Symposium on Naval Hydrdynamics*. 1997: Trondheim, Norway.

[3.] Oger, G., et al., *Two dimensional SPH simulations of wedge water entries.* Journal of Computational Physics, 2006. **213**(1): p. 20.

[4.] Kleefsman, K.M.T., et al., *A Volume-of-Fluid based simulation method for wave impact problems.* Journal of Computational Physics, 2005. **206**: p. 31.

[5.] Mojo, S., *Hydrodynamic interaction of horizontal circular cylinders with a free surface*. 1997, Brunel University: London.

[6.] Yan, S. and Q.W. Ma, *Numerical simulation of fully nonlinear interaction between steep waves and 2D floating bodies using the QALE-FEM method.* Journal of Computational Physics, 2007. **221**: p. 27.

[7.] Zhao, R. and O. Faltinsen, *Water entry of two dimensional bodies.* Journal of Fluid Mechanics, 1993. **246**: p. 20.

[8.] Gringold, R. and J.J. Monaghan, *Smoothed Particle Hydrodynamics: Theory and application to non-spherical stars.* Monthly Notices of the Royal Astronomical Society, 1997. **181**: p. 14.

[9.] Lucy, L., *A numerical approach to testing of the fusion process.* Astronomical Journal, 1997. **88**: p. 12.

[10.] Dalrymple, R.A., *Using Smoothed Particle Hydrodynamics for Waves*, in *Asian and Pacific Coasts*. 2007: Nanjing, China.

[11.] Monaghan, J.J., *Simulating Free Surface Flows with SPH.* Journal of Computational Physics, 1994. **110**: p. 8.

[12.] Monaghan, J.J., *SPH without a Tensile Instability.* Journal of Computational Physics, 2000. **159**: p. 22.

[13.] Monaghan, J.J., *On the problem of penetration in particle methods.* Journal of Computational Physics, 1989. **82**(1): p. 15.

[14.] Dyka, C.T. and R.P. Ingel, *An approach for tension instability in smoothed particle hydrodynamics (SPH).* Computers & Structures, 1995. **57**(4): p. 8.

[15.] Dyka, C.T., P.W. Randles, and R.P. Ingel, *Stress points for tension instability in SPH.* International Journal for Numerical Methods in engineering, 1997. **40**(13): p. 17.

[16.] Gomez-Desteira, M. and R.A. Dalrymple, *Using a 3D SPH method for wave impact on a tall structure.* Journal of Waterway, Port, Coastal and Ocean Engineering, 2004. **130**(2): p. 7.

[17.] Dalrymple, R.A. and B.D. Rogers, *Numerical modeling of water waves with the SPH method.* Coastal Engineering, 2006. **53**: p. 7.

[18.] Rogers, B.D. and R.A. Dalrymple. *SPH Modeling of Breaking waves*. in *ICCE*. 2004. Lisbon, Portugal: ASCE.

[19.] Morris, J.P., *Analysis of SPH with applications*. 1996, Monash University: Melbourne, Australia.

[20.] Colagrossi, A. and M. Landrini, *Numerical simulation of interfacial flows by smoothed particle hydrodynamics.* Journal of Computational Physics, 2003. **191**(1): p. 28.

[21.] SPHERIC, *SPHERIC Home Page*. 2008, University of Manchester.

[22.] Campbell, J.C., R. Vignjevic, and M. Patel, *A Coupled FE-SPH approach for Simulation of Structural Response to Extreme Wave and Green Water Loading*, in *Offshore Technology Conference*. 2008: Houston, Texas.

[23.] Greenhow, M., *Wedge Entry into initially calm water*. Applied Ocean Research, 1987. **9**(4): p. 10.

[24.] Zhao, R. and O. Faltinsen, *Water entry of arbitrary two-dimensional bodies.* Journal of Fluid Mechanics, 1993. **246**(1): p. 20.

[25.] Cointe, R., *Two-dimensional water-solid impact.* Journal of Offshore Mech. Artic Eng., 1987. **111**(1): p. 5.

[26.] Judge, C., A. Troesch, and M. Perlin, *Initial water impact of a wedge at vertical and oblique angles.* Journal of Engineering Mathematics, 2004. **48**(1): p. 25.

[27.] Greenhow, M. and S. Moyo, *Water entry and exit of horizontal circular cylinders.* Phil. Trans. R. oc. Lond., 1997. **335**(A): p. 13.

[28.] Rogers, B.D., et al. *Comparison and Evaluation of Multi-phase and Surface Tension models*. in *4th SPHERIC Workshop*. 2009. Nantes, France.

[29.] Shao, S. and E. Y.M.Lo, *Incompressible SPH method for simulating Newtonian and non-Newtonian flows with a free surface.* Advances in Water Resources, 2003. **26**(7): p. 14.